

Developing Remote Sensing Capabilities for Meter-Scale Sea Ice Properties

Chris Polashenski, PI
USACE-CRREL Building 4070
Fort Wainwright, AK 99703
phone: (570) 956-6990 fax: (907) 361-5188 email: christopher.m.polashenski@usace.army.mil

Award Number: N0001413MP20144

Karen E. Frey, co-PI
Graduate School of Geography, Clark University
950 Main Street
Worcester, MA 01610
phone: (508) 793-7209; email: kfrey@clarku.edu

Award Number: N000141310440

LONG-TERM GOALS

The overarching goal of this work is to develop and validate remote sensing techniques to track sea ice physical properties of geophysical importance that occur below the pixel size of most global-coverage satellite assets, particularly melt ponds.

OBJECTIVES

We will collect a dataset of high resolution satellite imagery and develop and field-validate methods for detecting melt pond area fraction, floe size distribution, and ice surface roughness from this imagery at a number of sites in the Arctic. The primary objective, in years 1 and 2, is to demonstrate the capability for operationally monitoring these variables. In the 3rd and 4th years of the project, these measurements will be scaled up to basin scale estimates, using both interpolation between observation sites and improved spectral mixing techniques to classify the fractional mixture of surface types within low resolution remote sensing imagery pixels, such as MODIS.

APPROACH

Key Participants:

Chris Polashenski (Research Geophysicist, ERDC-CRREL)
Elias Deeb (Research Scientist, ERDC-CRREL)
Karen Frey (Associate Professor, Clark University)
Don Perovich (Research Geophysicist, ERDC-CRREL)
Blaine Morris (Research Scientist, ERDC-CRREL)

| Report Documentation Page | | | Form Approved OMB No. 0704-0188 | | |
|--|------------------------------------|-------------------------------------|---|---|---------------------------------|
| Public reporting burden for the collection of information is estimated to average 1 hour per response, including the time for reviewing instructions, searching existing data sources, gathering and maintaining the data needed, and completing and reviewing the collection of information. Send comments regarding this burden estimate or any other aspect of this collection of information, including suggestions for reducing this burden, to Washington Headquarters Services, Directorate for Information Operations and Reports, 1215 Jefferson Davis Highway, Suite 1204, Arlington VA 22202-4302. Respondents should be aware that notwithstanding any other provision of law, no person shall be subject to a penalty for failing to comply with a collection of information if it does not display a currently valid OMB control number. | | | | | |
| 1. REPORT DATE 30 SEP 2014 | | 2. REPORT TYPE | | 3. DATES COVERED 00-00-2014 to 00-00-2014 | |
| 4. TITLE AND SUBTITLE Developing Remote Sensing Capabilities for Meter-Scale Sea Ice Properties | | | 5a. CONTRACT NUMBER | | |
| | | | 5b. GRANT NUMBER | | |
| | | | 5c. PROGRAM ELEMENT NUMBER | | |
| 6. AUTHOR(S) | | | 5d. PROJECT NUMBER | | |
| | | | 5e. TASK NUMBER | | |
| | | | 5f. WORK UNIT NUMBER | | |
| 7. PERFORMING ORGANIZATION NAME(S) AND ADDRESS(ES) U.S. Army Corps of Engineers,Cold Regions Research and Engineering Laboratory,Building 4070,Fort Wainwright,AK,99703 | | | 8. PERFORMING ORGANIZATION REPORT NUMBER | | |
| 9. SPONSORING/MONITORING AGENCY NAME(S) AND ADDRESS(ES) | | | 10. SPONSOR/MONITOR'S ACRONYM(S) | | |
| | | | 11. SPONSOR/MONITOR'S REPORT NUMBER(S) | | |
| 12. DISTRIBUTION/AVAILABILITY STATEMENT Approved for public release; distribution unlimited | | | | | |
| 13. SUPPLEMENTARY NOTES | | | | | |
| 14. ABSTRACT | | | | | |
| 15. SUBJECT TERMS | | | | | |
| 16. SECURITY CLASSIFICATION OF: | | | 17. LIMITATION OF ABSTRACT Same as Report (SAR) | 18. NUMBER OF PAGES 19 | 19a. NAME OF RESPONSIBLE PERSON |
| a. REPORT unclassified | b. ABSTRACT unclassified | c. THIS PAGE unclassified | | | |

Carolyn Stwertka (Graduate Student, Thayer School of Engineering, Dartmouth College)

Alexandra Arntsen (Graduate Student, Thayer School of Engineering, Dartmouth College)

Christie Wood Logvinova (Graduate Student, Clark University)

Nelson Crone (Graduate Student, Clark University)

Justin Chen (High School Student, Hanover High School)

Key Tasks:

1. Task and acquire high resolution panchromatic and multispectral optical (e.g. Quickbird, Worldview, National Assets) and synthetic aperture radar (TerraSAR-X, COSMO-SkyMed, or RADARSAT-2) images of regionally representative ~10x10km test areas (Yr 1–4)
2. Collect in situ measurements of target variables for validation of data products derived from high resolution satellite assets, using surface based observations and aerial photography at three readily accessible sites. (Yr 1–2)
3. Develop and validate automated pixel classification algorithms to extract pond coverage, floe size distribution, and ice surface roughness from high resolution satellite assets, and use these algorithms to create data products at sample sites distributed around the Arctic. (Yr 1-2)
4. Further develop and validate algorithms to derive melt pond coverage and floe size distribution from lower resolution assets through techniques such as spectral mixing based on in situ spectral measurements. (Yr 2–4)
5. Rapidly disseminate all data products created, along with suitable metadata, and publish methodology developed. (Yr 1–4)

WORK COMPLETED

During 2014 we built upon our successes capturing imagery; developed, tested, and iterated methods to segment and classify the imagery; arrived at a stable processing methodology; and began mass-processing imagery. With these accomplishments, we have now achieved a high level of success in key tasks 1,3, and 4. We also took significant steps toward conducting in situ validation of our methods (task 2), though without yet achieving our goals. We recognize the need to enhance our distribution of our data and methodology (task 5) now that we have begun producing useful products and have submitted abstracts and begun papers which will enable us to report success on this task in FY2015. Overall we are very pleased to report that the project is on schedule and making clear progress in meeting its overall goals. Below we detail our work efforts as organized around these five key tasks.

Task 1 - Imagery Acquisition

We have worked with a wide variety of partners to task and acquire optical and radar imagery tracking both fixed sites and drifting sites throughout the Arctic. Based on utility, our primary focus has narrowed to multispectral optical imagery during FY14. Though we are still working with both radar and panchromatic NTM imagery, our acquisition efforts have moved away from these imagery types somewhat. We have been able to collect a great imagery dataset that includes sample sites across most of the Arctic basin and spans a broad range of sea ice concentrations and melt pond coverage, both across space and time. Our imagery library is now over 3,000 images and large enough for us to begin assessing the spatial and temporal variation of key variables at many of the sites we are tracking.

Commercial Optical Imagery

This year we focused on improving the success of our commercial optical imagery acquisitions to increase the number of cloud-free scenes acquired. Multispectral, high resolution imagery from Quickbird and Worldview 2 has proven to be by far the most suitable for automated identification and classification of sea ice surface conditions. As a result, we dropped acquisitions from Worldview 1 (panchromatic only) and tasked imagery exclusively from Worldview 2 and Quickbird. Once again we attempted to track the temporal evolution at both fixed locations and drifting sites. Based on summer 2013 tasking results and prevalence of clouds in optical satellite collections, a new requirement was developed in collaboration with the Polar Geospatial Center (PGC) through the National Geospatial Intelligence Agency (NGA) to direct the commercial satellite vendor (Digital Globe) in tasking their platforms toward the acquisition of twenty (20) identified fixed sites every three (3) days regardless of cloud cover (Figure 1). Last year's collections, requested once in every two week period when the vendor's algorithms determined the scene was cloud free, resulted in excessive collection of cloudy imagery. The vendor's proprietary methodology for determining cloud-free scenes apparently was not functioning correctly over sea ice, and in fact collected cloudy scenes at a rate significantly higher than climatology would predict. By switching to a higher frequency of acquisition and removing the black box of the vendor's filter, the anticipated result was that many more collections would be made over each fixed site with the hopes that more relatively cloud-free opportunities would be acquired, simply mirroring the cloud free percentage of the areas.

Overall, this strategy was much more successful. Table 1 shows the results of the collection strategy for the twenty (20) fixed sites between 6/1/2014 and 9/8/2014. The number of collections with cloud cover less than 25% has dramatically increased from last year. Successful, cloud free, collections now average weekly rather than roughly every three weeks. We are pleased with these results and feel that we can now track the temporal evolution of key sea ice surface characteristics at fixed sites well.

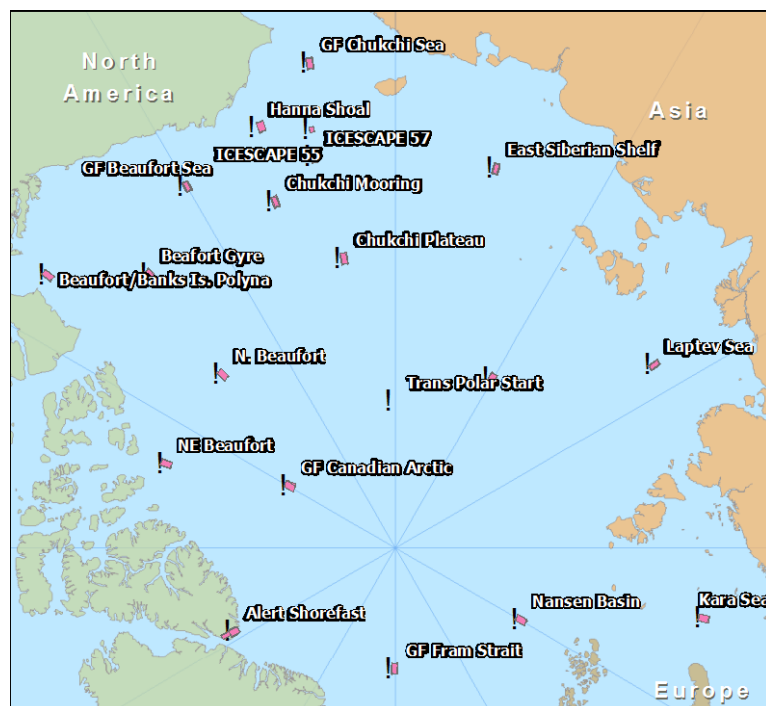


Figure 1 – Digital Globe 2014 collection results for twenty (20) Arctic fixed sites for the period of 6/1/2014 through 9/8/2014. Magenta polygons represent boundaries of collected scenes.

Table 1 – Digital Globe 2014 collection results for twenty (20) Arctic fixed sites for the period of 6/1/2014 through 9/8/2014 and the number of scenes identified as having less than 25% cloud cover. Magenta polygons represent boundaries of collected scenes.

| Fixed site name | Latitude | Longitude | # collections | # collections < 25% clouds |
|------------------------|-----------------|------------------|----------------------|--|
| Alert Shorefast | -62.3 | 82.5 | 86 | 27 (31%) |
| Beafor Gyre | -138 | 75 | 63 | 21 (33%) |
| Beaufort/Banks Is. | -128 | 72 | 73 | 17 (23%) |
| Chukchi Mooring | -160.9 | 75.1 | 76 | 15 (20%) |
| Chukchi Plateau | -170 | 78 | 114 | 13 (11%) |
| East Siberian Shelf | 165 | 74 | 48 | 11 (23%) |
| GF Beaufort Sea | -150 | 73 | 62 | 17 (27%) |
| GF Canadian Arctic | -120 | 85 | 74 | 18 (24%) |
| GF Chukchi Sea | -170 | 70 | 68 | 13 (19%) |
| GF E Siberian Sea | 150 | 82 | 112 | 15 (13%) |
| GF Fram Strait | 0 | 85 | 71 | 16 (23%) |
| Hanna Shoal | -161.9 | 72.0 | 8 | 1 (13%) |
| ICESCAPE 55 | -168.7 | 72.6 | 9 | 2 (22%) |
| ICESCAPE 57 | -168.3 | 73.7 | 80 | 14 (18%) |
| Kara Sea | 77 | 77 | 80 | 3 (4%) |
| Laptev Sea | 125 | 77 | 92 | 8 (9%) |
| N. Beaufort | -135 | 80 | 50 | 12 (24%) |
| Nansen Basin | 60 | 84 | 81 | 22 (27%) |
| NE Beaufort | -110 | 80 | 89 | 21 (24%) |
| Trans Polar Start | -180 | 84 | 0 | N/A |

Note: collections for the Trans Polar Start fixed site are currently not feasible based on issues with the commercial satellite vendor's ability to task collections in close proximity to the geographic North Pole.

In addition to the fixed sites, throughout the Summer 2014 season, nine (9) CRREL ice mass balance buoys were targeted on an approximately bi-weekly basis using commercial high-resolution satellite imagery to achieve a lagrangian view of the ice. Table 2 highlights the dates of submitting tasking requirements. Figure 2 geographically shows the drift tracks of the current six (6) CRREL ice mass balance buoys and satisfied requirements for commercial satellite collections from 5/1/2014 through 9/8/2014. These targets represent 265 satisfied collection requirements with 61 (23%) collections having less than 25% cloud cover.

Table 2. Submission of 2014 tasking requirements for optical high-resolution commercial collections. Buoy names reflect the CRREL ice mass balance buoy targeted.

See <http://imb.crrel.usace.army.mil/newdata.htm> for current locations. Note:

Vendor ability to satisfy collection requirement dictated by several factors (e.g. cloud-cover percentage, collection competition, and satellite vendor issues collecting targets in close proximity to geographic North Pole).

| | 2012G | 2013F | 2013G | 2013I | 2014B | 2014C | 2014D | 2014E | 2014F |
|-----------|-------|-------|-------|-------|-------|-------|-------|-------|-------|
| 5/5/2014 | X | X | X | X | X | X | X | X | |
| 5/21/2014 | X | X | | X | X | X | X | X | |
| 6/3/2014 | X | X | | X | X | X | X | X | |
| 6/23/2014 | X | X | | | X | X | X | X | |
| 7/21/2014 | X | X | | | X | X | | X | |
| 8/4/2014 | X | X | | | X | X | X | X | |
| 8/21/2014 | X | X | | | X | X | | X | X |
| 9/2/2014 | X | X | | | X | X | | X | X |

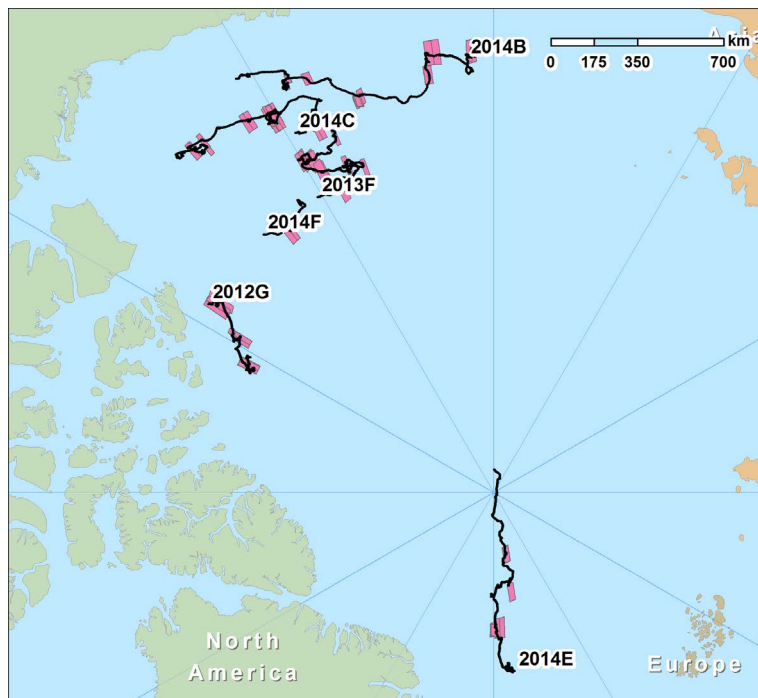


Figure 2 - Digital Globe 2014 collection results for the current six (6) CRREL sea ice mass balance buoys from 5/1/2014 through 9/8/2014. Magenta polygons represent boundaries of collected scenes.

Declassified National Technical Means Imagery

With collaborating ONR projects leading the collection of NTM and radar imagery we reduced our efforts to expand collection of these imagery types. Instead we sent shapefiles and copies of our commercial imagery collection plans to others (i.e. MEDEA, Rob Graydon, Hans Greber), and modified our plans to collect as much coincident data as possible. The NTM imagery being collected has been highly successful at executing rapid repeats (every few days) of sites being tracked and in this regard has been superior to our abilities to track lagrangian sites. The key benefit of the NTM imagery, therefore, is the ability to temporally infill multispectral imagery collected through the commercial vendors – we’ve responded to this utility by coordinating our sites to match the MEDEA and MIZ sites as closely as possible. Simultaneous collection of panchromatic and multispectral Worldview 2 imagery is allowing us to intercompare methods being developed by project N0001413MP20163 for NTM processing with results from our multispectral collections on the same scenes.

Commercial Radar imagery

Though radar imagery was not the central focus of this program, we have collected a number of RADARSAT scenes, collaborated with Phil Hwang at SAMS to get a number of TerraSAR-X images (~200) of our sites and worked with NGA to conduct a time series of acquisitions with COSMO-SkyMed at our Beafort Sea fixed site approximately every 10 days. Preliminary investigation of these data is discussed below.

Task 3 – Develop Imagery Processing Techniques

a. Optical Imagery Processing

We have iterated and tested numerous algorithms to segment and classify optical imagery, using a combination of both off the shelf software such as ENVI, Imagine, ArcGIS, and IDL, and implementing our own algorithms in Matlab. We have identified an algorithm that produces high accuracy segmentation and classification and completed a workflow design that we are now implementing in mass-processing imagery.

Arriving at a workable methodology has not been straightforward. Our efforts in FY13 showed that our proposed methodology for processing the imagery to identify surface types - using calibrated spectral albedo measurements from prior field work for different surface types to create a library of surface spectral signatures to be used in a multivariable thresholding scheme was an inadequate approach. The intensity values have significant overlap in regions between very bright melt ponds and dirty sea ice, as well as between very dark melt ponds and open water. Even with spectral imagery, therefore, single pixel differentiation by spectral thresholding or band ratios showed classification accuracy of only 70-80%. These techniques lie at the core of recent developments in lower resolution remote sensing of ponds using MODIS (i.e. Rosel et al., 2014) raising serious questions about the accuracy of these derivations that we have begun explore below by intercomparison of MODIS derived pond coverage with Worldview derived statistics.

During FY2014 we implemented and tested the performance of several more sophisticated algorithms. Examples include a thresholding plus minimum distance classification which identifies pixels with band ratios in the center of the expected spectral signature space, then clusters the remaining ambiguous pixels based on an iterative minimum distance technique similar to voter-type algorithms and K-means segmentation coupled with a maximum likelihood classification. The results of these intermediate complexity efforts were better than simple thresholding, but produced classification accuracy of only ~80%-90% - still inadequate for our purposes.

The method we've settled on uses a multitude of feature characteristics, rather than just color intensity to segment the image into objects and then classify these objects into categories. We implement this using the feature extraction module of ENVI with a random forest classifier run in matlab, similar to methods proposed by Miao et al., 2014 for aerial imagery processing. The feature extraction module of ENVI breaks down the image into a series of segments along boundaries in chosen characteristics. Selecting the scale and merge values for the ENVI feature extraction module has been an iterative process, and ensuring that feature boundaries appear at all physically important locations requires breaking down the image into segmentation objects smaller than the typical surface feature (i.e. melt pond) size. Recombining adjacent cells of like type later in the processing allows us to make features whole again.

After segmentation in the ENVI feature extraction module, statistics of each object, including its color and brightness, but also shape, tortuosity, texture, variability, etc are then calculated. The expanded set of characteristic variables has greatly helped us differentiate between spectrally similar areas in multispectral imagery. For example, dark melt ponds with thin ice at the bottom lose their blue hue and are spectrally challenging to distinguish from open water. The ponds however have higher intensity variance and can be reliably differentiated using textural parameters.

Machine learning is used to develop a classification scheme for the multivariate problem. Hundreds of segments in images selected from across the entire range of seasonal ice conditions are manually identified as a training set and from these we create random forest classifier trees. The random forest classifier is then run on numerous images. The more similar the images are to the training set, naturally the better the results, but results have proven very good across the entire summer season using only a single training set. An example image being taken through this workflow is presented in Figure 3 and accuracy matrices are presented in Table 3. This image is typical of our classification success, showing user and producer accuracy well above the 90%; 94.5% in this case. Accuracy in this case is determined by randomly selecting several hundred segments (see Figure 4 for a sample area), identifying these visually by human eye, and comparing the human classification to the machine classification.

Once we settled on a segmentation and classification scheme we recognized that a large portion of the remaining error comes from the hard-to-classify edge pixels which span the boundary between surface types. To reduce the area of the image that is covered by edge pixels, we have also incorporated pansharpening into our workflow to further enhance our ability to resolve fine scale features. This methodology combines the intensity values from the higher resolution panchromatic WV2 imagery with the color information from the multispectral coincident image to create a multispectral imagery product at the resolution of the panchromatic product, providing us the opportunity to carry out our methods on a much finer scale. There are many types of pansharpening algorithms and we conducted tests to see which produces the highest improvement in classification accuracy. Because of the strong role textural characteristics play in classification, we found that methods which better preserve texture rather than color are best. (see Figure 5)

Scale to Production

With our methodology development at a stable version state, we've begun refining and scripting the workflow (below) to mass-process the imagery and exploring ways to combine our methodology into fewer software packages. Processing time is currently substantial at approximately 2 hours per image on an 8-core machine. Though we've processed ~200 images, more work is necessary to streamline our process, our current processing time does not permit us to keep up with acquisition rates. In recent

weeks, we've also purchased a more powerful workstation computer (using overhead funds to ensure compliance with the ONR directives) and added a step to our workflow which splits the imagery into tiles for processing, thereby reducing RAM needs, and recombines them after completion. We expect that with additional effort toward efficiency we will be able to reduce processing time for an image to several minutes. Finally, partial cloud cover, surface shadowing, and streaking in many images preclude accurate classification. Up to this point our work has only included the manually selected or masked clear sky images. We plan to develop automated detection for some of these imagery flaws during the coming year, but for now are simply manually selecting clear sky imagery.

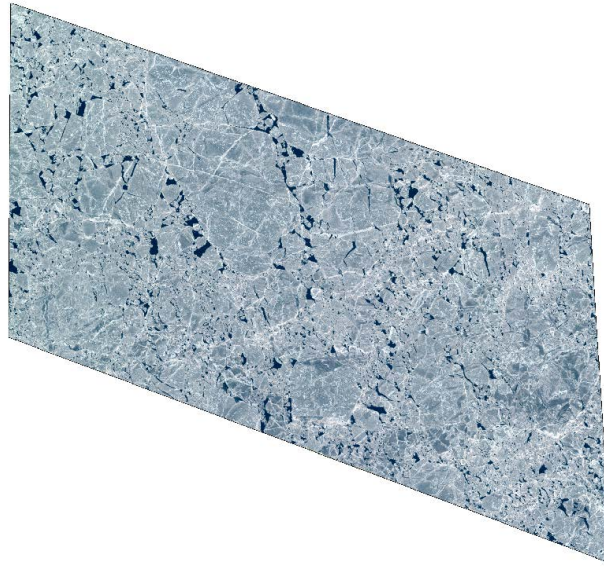
Current workflow:

1. Collect images (generally in NITF format)
2. Manually identify clear sky imagery (ENVI)
3. Orthorectify images (IDL/ENVI)
4. Pan sharpen imagery (IMAGINE)
5. Tile images (IDL/ENVI)
6. Conduct Feature Extraction (IDL/ENVI)
 - 6a. Create training dataset and build a random forest trees (MATLAB).
7. Execute Random Forest Classifier (MATLAB)
8. Merge like Features (ARCGIS/Python)
9. Calculate statistics and archive result image (MATLAB).

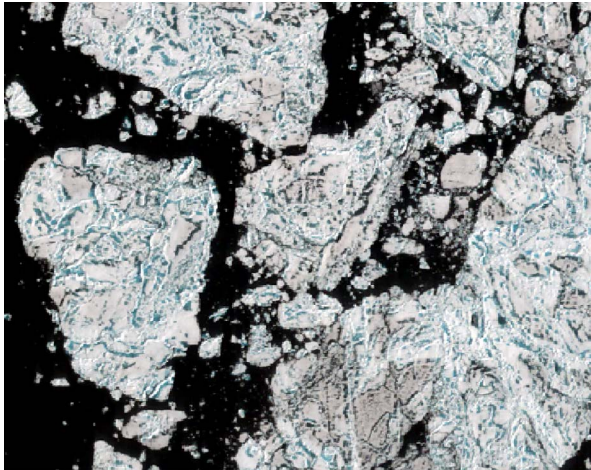
Table 3 - The error matrix for the image presented in Figure 3. Note that overall user accuracy (the likelihood that any point on the image is correctly labeled) is good at 94.5%, but that melt ponds were sometimes miss-classified. This is partly due to edge pixels of melt ponds being miss-classified. Classification of melt ponds in this image improved slightly when pan sharpened.

| | Ground Reference | | | | | | |
|---------------------|------------------|-----------|-------|----------|----------|-------|-----------------|
| | Water | Melt Pond | Ridge | Bare Ice | Brash | Total | User's Accuracy |
| Water | 24 | 0 | 0 | 0 | 1 | 25 | 96 |
| Melt Pond | 0 | 19 | 0 | 0 | 0 | 19 | 100 |
| Ridge | 0 | 0 | 15 | 1 | 0 | 16 | 93.75 |
| Bare Ice | 0 | 6 | 0 | 142 | 1 | 149 | 95.30201342 |
| Brash | 0 | 4 | 0 | 0 | 24 | 28 | 85.71428571 |
| Total | 24 | 29 | 15 | 143 | 26 | 237 | |
| Producer's Accuracy | 100 | 65.51724 | 100 | 99.3007 | 92.30769 | | 94.51476793 |

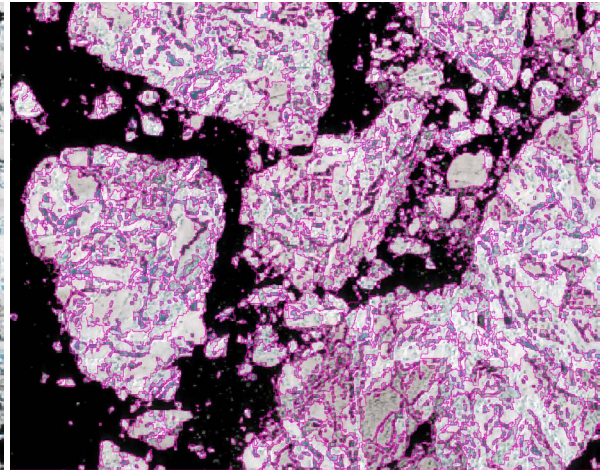
a.



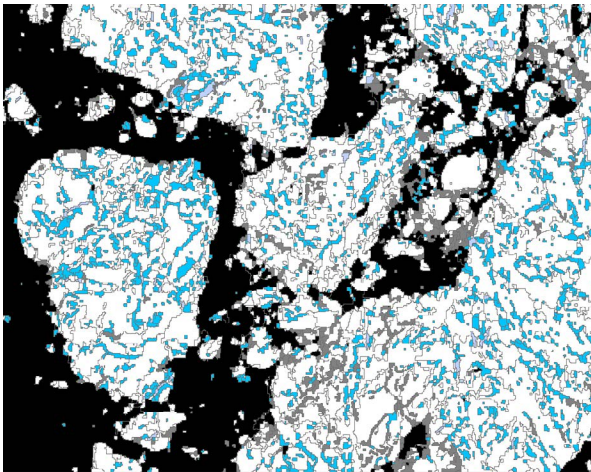
b.



c.



d.



e.

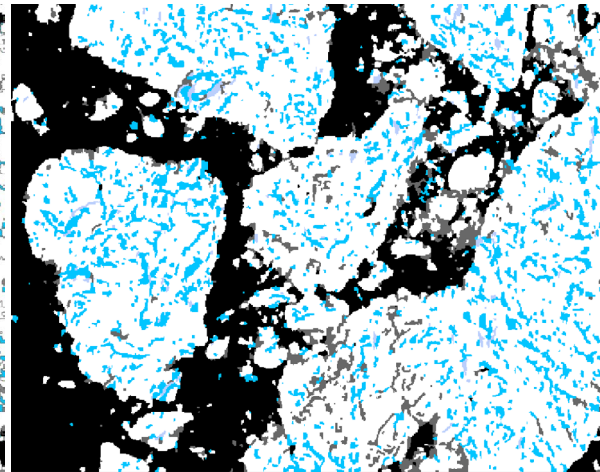


Figure 3. Sample sea ice image from July 10th at the Beaufort sea site (a.) and a zoomed in look at a subset of this image (b.), being segmented using the ENVI feature extraction module, (c.), having the segments classified using our Matlab implementation of a random forest classifier (d.), and having adjacent segments merged together to create a final image. In the final image, blue is melt ponds, purple is ridged ice, and gray is brash ice. Overall accuracy of this image classification was 94.5%, compared to a human classifier.

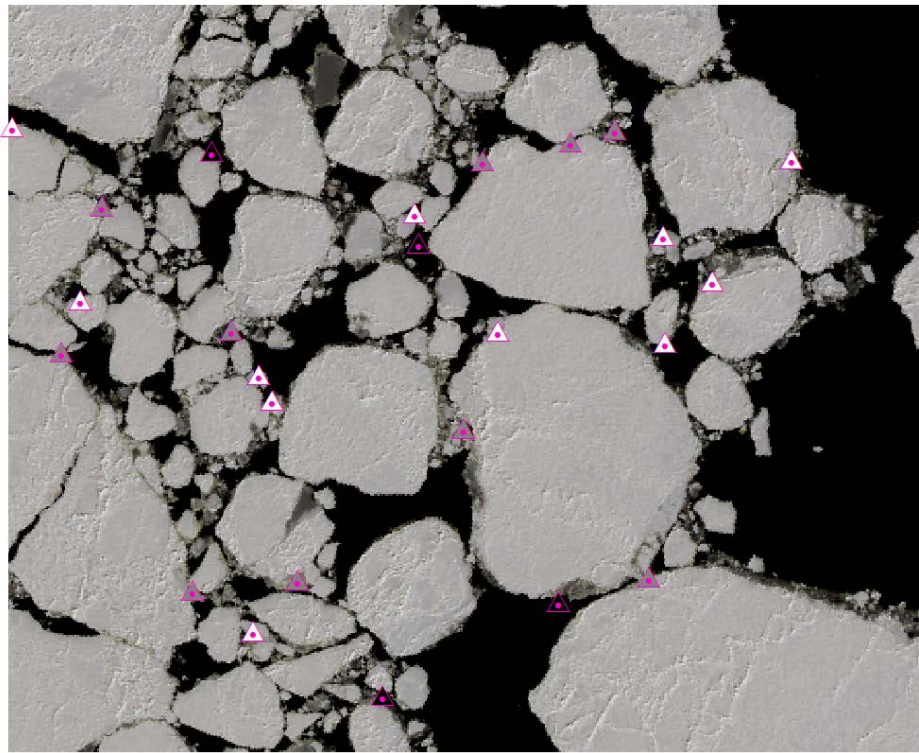


Figure 4. An image from May 11th at the Beaufort Sea site showing our validation methodology. Object locations are randomly selected for human classification. Comparison between the human classification of the points and the machine classification is used to validate our methodology.

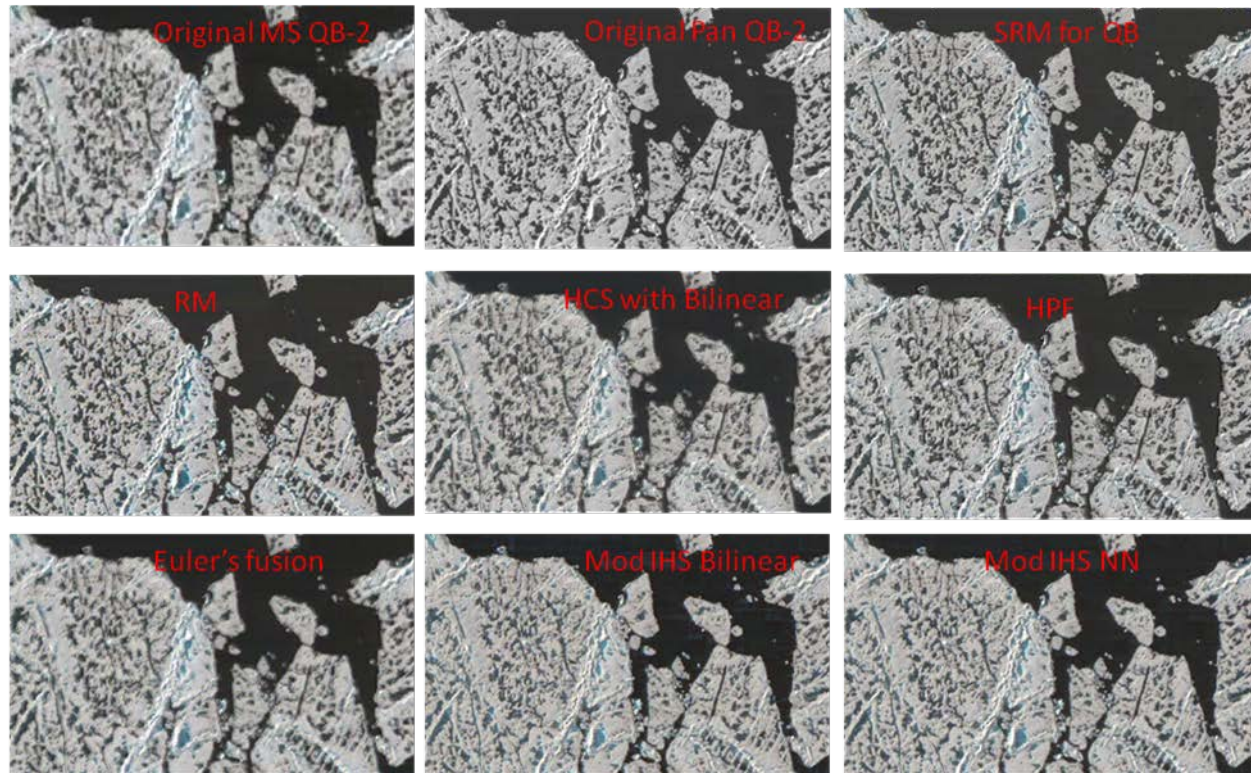


Figure 5 – Sample of pan sharpening results from different methodologies. Original multispectral image top left, original panchromatic image, top center. We selected SRM methodology for its highest detail definition, even though its color performance was inferior to RM or Mod IHS.

b. Radar Imagery Processing:

In addition to our work on optical imagery, we've carried out some work on basic processing of radar imagery from Radarsat-2, which we can also apply to our CosmoSkyMed and TerraSAR-X collections in the coming year. Radarsat-2 carries a C-band (5.405 cm) synthetic aperture radar (SAR) with multiple polarization and capture modes. This study used HH-polarized, 50 meter resolution scenes from the Beaufort Sea, collected in June, 2014.

Filtering

Backscatter values over sea ice and water range from near 0 to 100 (8-bit integer); however, multiplicative noise or speckle, caused by interference in signal return processing, can produce anomalous backscatter values up to 50% higher or lower than a pixel's appropriate value. To mitigate these effects, an adaptive filter (Frost *et al.*, 1982) was applied using a 7x7 pixel moving window (top two panels, Figure 6)—a 7x7 window (350 x 350 m) was chosen for this particular data set based upon its successful removal of noise and minimal signal degradation along a random transect as compared to a range (3x3 to 15x15) of other windows.

Histogram Analyses and Classification

To delineate between land-cover classes (water, ice, and various mixtures and interactions of water and ice), we assume that each class is represented by a normally distributed range of backscatter values

around some mean. The relative magnitude (counts) and mean backscatter value for each class varies widely by scene depending on land-cover and sensor geometry, respectively. In an individual scene's backscatter histogram, superimposed classes can be separated by identifying areas of positive curvature in the histogram (Figure 7). Backscatter thresholds (black lines in Figure 7) were assigned based upon the midpoints of the adjacent negative curvature areas in counts vs. backscatter (histogram) space.

Interpretation and Multi-scene Application

While the relationship between land-cover types and classes can be assigned manually on a by-scene basis, automatic assignment of classes requires more information. An empirical relationship exists between viewing angle and backscatter (Zakhvatkina *et al.*, 2013), but the viewing geometry of these collections is unavailable. Scene-to-scene class registration may be possible by leveraging the characteristic length-scales of different land-cover types using an object-oriented classifier or image-segmentation technique—for example, automatically identifying areas of highly fractured ice based on the relatively short length-scale of its constituent parts in two different scenes could allow the user to identify areas of lower (water) and higher (ice) backscatter in both images, despite the average backscatter values of each being different.

Results

Initial application of the classification methods to multiple (25) scenes show positive results; however, inability to automatically link classes and land-cover types between scenes prevents full automation of the process. Level set methods (Osher & Fedkiw, 2002) are being investigated as both an alternative filtering method and means of image segmentation/object delineation. Application of these methods attempt to create level sets or iso-contours, lines of equal backscatter by filtering small-scale variability in a given window around each pixel. Subsequent iterations degrade the backscatter signal but increase the size of regions of equal backscatter, smoothing the image (Figure 6, panel 4). Regions with high backscatter gradients, usually corresponding to the ice-water interface, are least affected. While this preserves edges and allows for easy identification of floes surrounded by clear water, low-gradient regions may be adversely affected. The most appropriate methodology and application of these techniques for image filtering and assessment of individual flows or class-specific characteristic length scales will require further investigation.

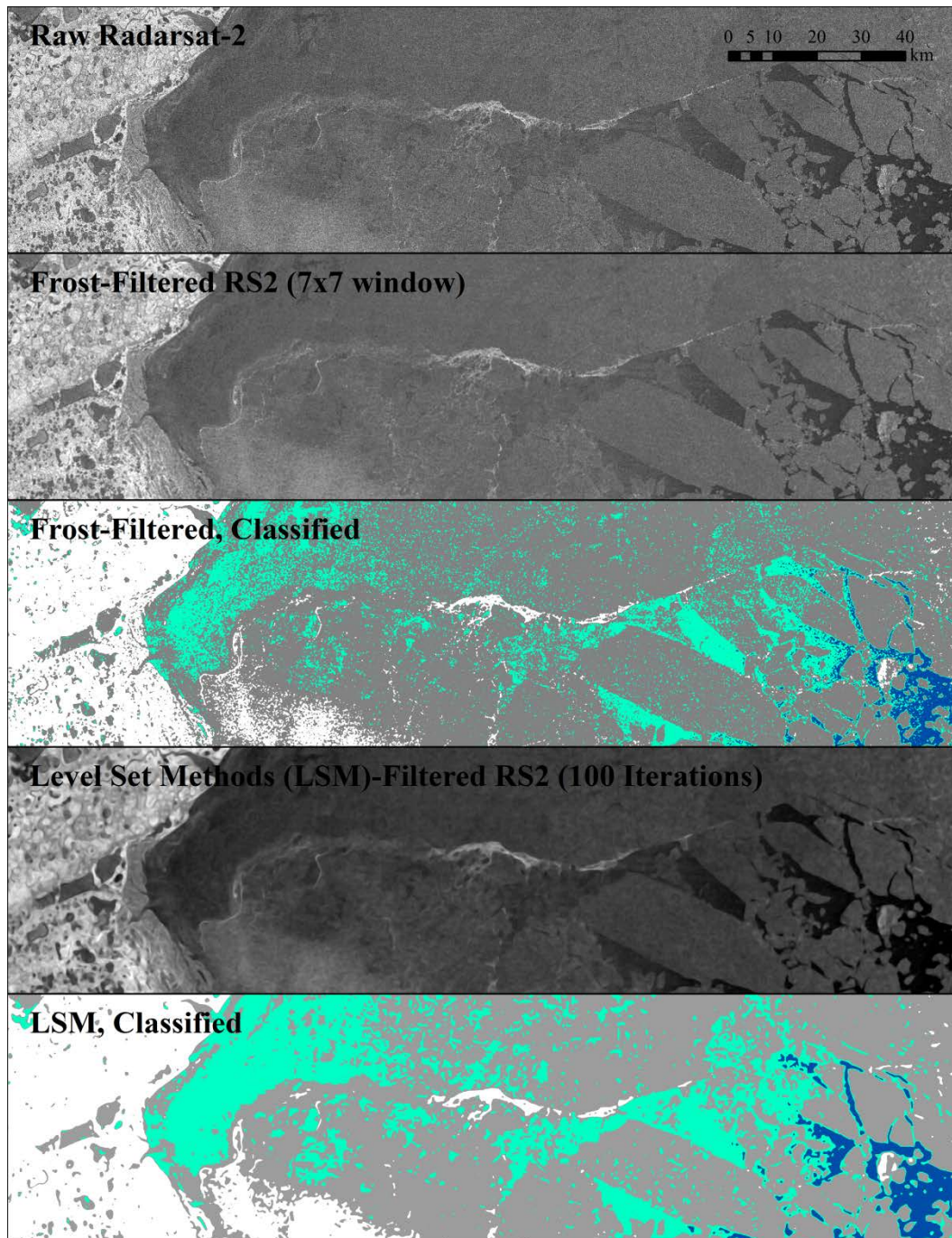


Figure 6. Examples of raw, filtered, and classified scenes. Panels show (1) the raw Radarsat-2 image, (2) the image after applying a 7x7 Frost filter, (3) the classified scene based on the Frost-filtered image, (4) the image after applying level set methods (LSM) using a 7x7 window over 100 iterations, and (5) the classified scene based on the LSM image. The histogram for this scene (from the full Frost-filtered image, not this subset) appears in Figure 2; the thematic maps in panel 3/5 show classes 1 and 2 as dark blue, 3 as cyan, 4 as grey, and 5 as white. Class merging and interpretation were done manually.

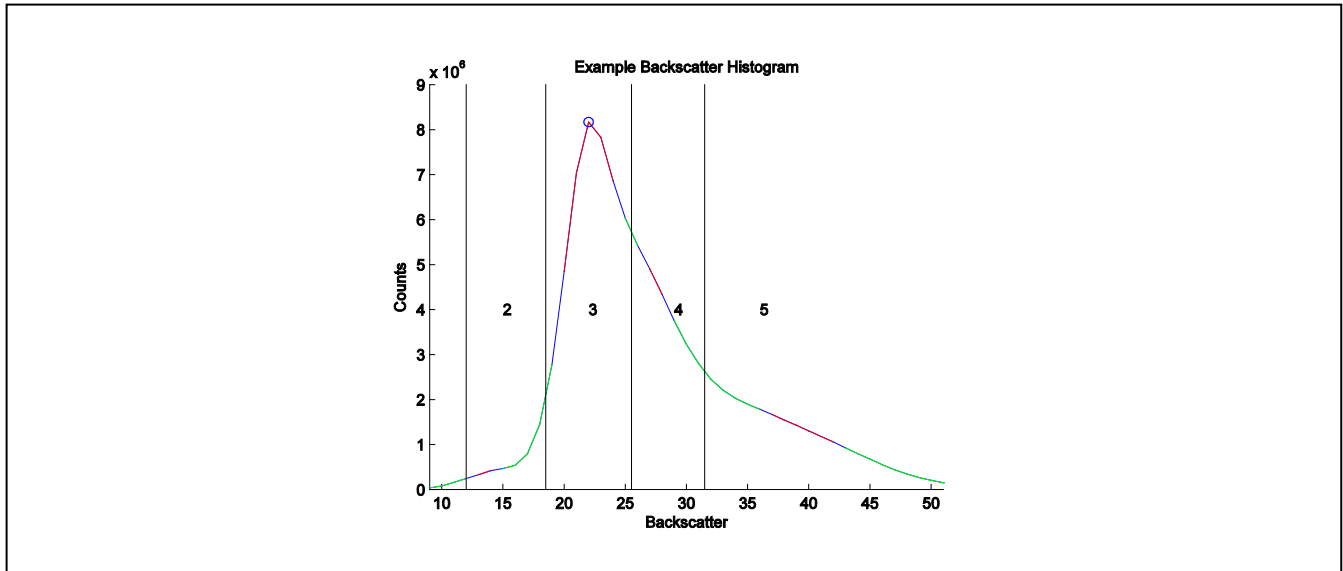


Figure 7. Example Scene Histogram (full scene from which Figure 1 is subset). By assuming that the backscatter of visibly separable materials (water, ice, mixtures) is normally distributed, individual classes can be identified by separating areas of positive curvature (red) within the histogram. Thresholds were assigned based upon the midpoint (in histogram space) of the adjacent negative curvature (green) regions. Blue regions represent inflection regions (rather than points due to integer binning).

Task 2 – Collect in Situ Data for Field Validation

Though visual validation of our algorithms against human classifiers has been conducted extensively, we also proposed to conduct field validation where we collected higher resolution aerial imagery and ground based measurements of pond locations to compare to our derived pond coverage. We attempted to carry out this work as part of the SUBICE (Study of Under ice Blooms In the Chukchi Ecosystem) Expedition aboard the USCGC Healy for about six weeks during May and June of 2014. Our results did not fully achieve our in-situ validation goals.

Our initial efforts involved collaborating with ACUASI – the UAV flight center at the University of Alaska Fairbanks to field several UAV packages from aboard Healy with the idea that we’d do numerous flights while the ship was in transit collecting aerial photomosaics coincident with tasking the ship track for Worldview imagery. Unfortunately Healy’s flight deck is governed by Navy rules which did not permit UAV landings on the ship (though paradoxically permitted takeoffs). Left with a greatly diminished opportunity for conducting flights while the ship was in motion, we reduced the scope of the UAV activities. Instead we purchased and a single hexacopter with camera system for our own efforts. Constrained to only flying the system when we were able to stop for an on-ice deployment, we were still optimistic we’d get at least a handful of coincident data collections.

The meteorological conditions, however, were very unfavorable for our plans to collect coincident satellite imagery, aerial imagery, and ground surveys. We made flights at 9 of 15 sites during the course of the cruise, covering a few square kilometers at each site. Melt was late, meaning that melt ponds did not form until the very end of our 7 week cruise, and persistent cloud cover throughout the

cruise meant that only one coincident UAV imagery collection/WV2 satellite scene were collected, and this one prior to the onset of melt. In this regard, we did not collect the data we require to do a high resolution validation. We do feel, however, that the significant effort we put into preparing the UAV system, imagery processing and mosaic routines, and pushing the Coast Guard to reconsider their UAV policies positions us much better for future opportunities.

Task 4 – Scale Up Using Lower Resolution Satellite Assets

MODIS-Based Melt Pond Analysis

An 8-day image time series of Arctic Ocean melt pond fraction on sea ice was created from MODIS surface reflectance for the years 2000–2011 by Rösel et al. (2012) and recently made publicly available. The advantage of this MODIS-based time series over other datasets (e.g., WorldView imagery) is the higher temporal resolution, reliability of continuous data collection over time, and more widespread spatial coverage. However, proper accuracy assessment and validation of this product has yet to occur. To this end, we are currently testing the accuracy of this new MODIS-based product in the Chukchi Sea by comparing the melt pond fraction in these images to the melt pond fraction in our resulting classified WorldView-02 imagery. We are additionally utilizing the MODIS product to look at spatial and temporal trends in melt pond fraction for the Chukchi Sea and surrounding regions. To date, we have acquired all available MODIS melt pond fraction imagery and begun to explore spatial and temporal trends. Figure 8 shows the changes in the MODIS melt pond fraction on sea ice over a seasonal cycle for the entire pan-Arctic for years 2002, 2007 and 2011. This figure illustrates some of the variation in the temporal and spatial distribution of melt ponds over for this time series. There is noticeably lower melt pond fraction in 2002, particularly in June, compared to 2007 and 2011. In 2007, an increase in melt pond fraction occurred in our study area in the Chukchi Sea (as well as in the Beaufort and Laptev Seas), whereas in 2011, higher melt pond fraction was concentrated in the southern parts of Beaufort Sea and Laptev Sea (as well as Baffin and Hudson Bay).

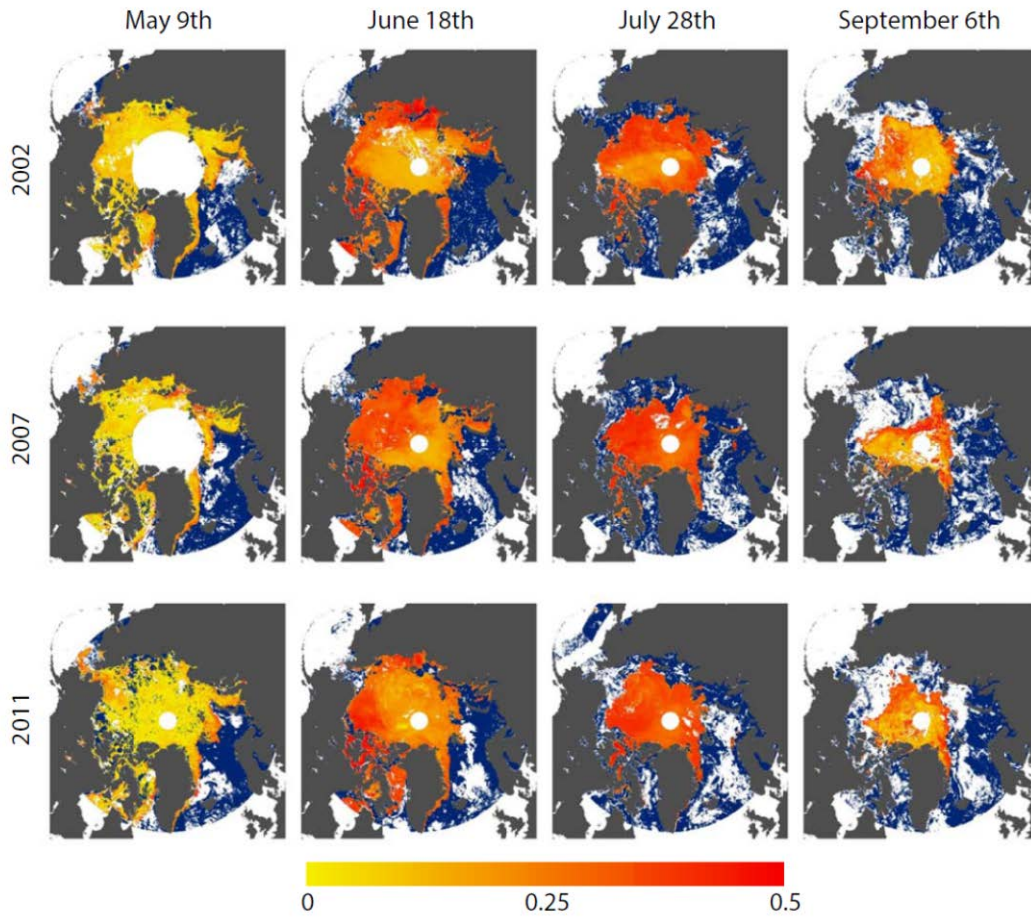


Figure 8. Seasonal cycle of the melt pond fraction on sea ice from MODIS satellite data (Rösel et al., 2012) across the pan-Arctic in 2002, 2007 and 2011. Dark blue areas indicate open water and white areas are data gaps. Melt pond fraction is displayed on a scale from yellow to red where yellow represents no melt ponds on sea ice and red represents greater than 50 percent melt pond fraction on sea ice.

Figure 9 shows examples of temporal profiles of melt pond fraction on sea ice in the Chukchi Sea. All three profiles were taken at the same location in the Chukchi Sea, which was located in the general vicinity of our WorldView-02 imagery. Noticeably higher melt pond fraction was observed in June and July of 2007 (also the same year with the lowest sea ice extent for this series). Open water (equivalent to zero melt pond fraction) occurred earlier in 2007 than in 2002 and significantly earlier in 2011. Looking at the beginning of the time series, 2011 had the highest starting melt pond fraction for this location. This suggests that melt pond formation may have begun earlier that year and which could have led to the earlier retreat of sea ice at this location. However, these time series are at fixed locations and do not account for sea ice movement. Temporal profiles of MODIS melt pond fraction for all years and all Worldview-02 imagery locations are currently being constructed. In addition, we will be performing more sophisticated image time series analysis to understand how melt pond distribution has changed both spatially and temporally over the past decade.

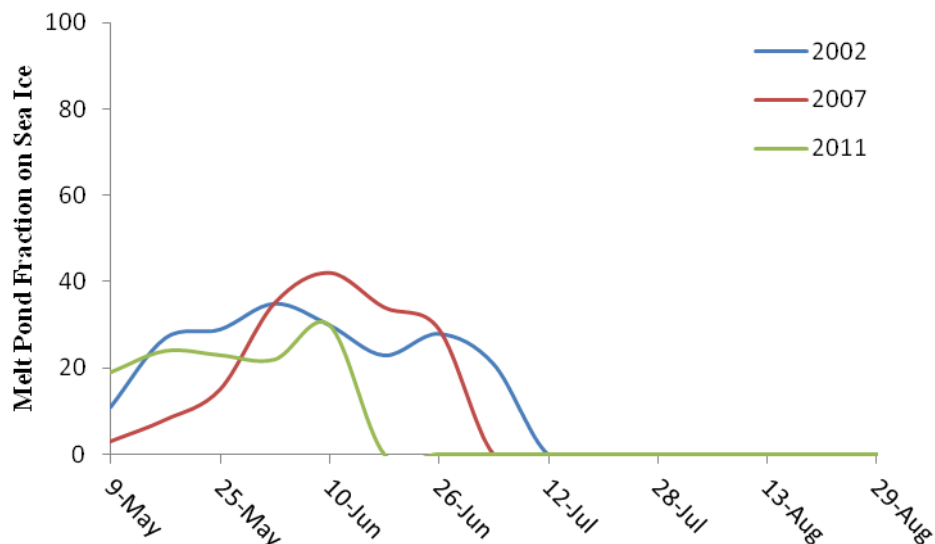


Figure 9. Example temporal profiles of melt pond fraction on sea ice in the Chukchi Sea in years 2002, 2007 and 2009 at the same location.

Task 5 – Disseminate Data and Methodology

We have submitted abstracts for the AGU fall meeting and begun preparing a paper on our methodology. We have also shared our imagery collection with collaborators on the ONR projects and will be packaging our processing scripts for sharing with other groups in coming months. Dissemination and technology transfer will come into higher focus during early FY15 now that we are comfortable with our methods.

RESULTS

We have:

- Collected a library of over 2,000 high resolution satellite images at both fixed and lagrangian sites throughout the Arctic Basin.
- Assembled the UAV equipment, photomosaic workflow, and imagery tasking protocols required to conduct field validation studies.
- Developed, tested, and validated a workflow for classifying surface types at meter scale in optical sea ice imagery.
- Begun mass-processing our imagery library.
- Shared our imagery library with several collaborators and begun writing publications on the methodology.

IMPACT/APPLICATIONS

The results of this study will include both a dataset of key meter-scale sea ice properties derived from our observation sites and the toolkit required to assess these properties in a uniform way from future imagery. This data and these techniques will enable synthesis activities seeking to explain the mechanisms and feedbacks governing ice loss in the Arctic. These synthesis activities are not

hypothetical – PI Polashenski has secured NSF funding for a 3 year project to integrate the remote sensing with in situ buoy data to quantify solar partitioning, and the products of this work are highly integrated with several other ONR projects listed above. To ensure our methodology developed can be used beyond this project we plan to release our processing scheme as a standardized shell script downloadable from our website in the coming months.

RELATED PROJECTS

We are coordinating efforts and sharing data with a suite of four closely related ONR projects:

N0001413MP20105: Propagation of Shortwave Radiation Through A Spatially Complex Melting Ice Cover – Lead PI Donald Perovich, USACE-CRREL

N0001413MP20102: Evolution of Melt Pond Geometry on Arctic Sea Ice – Lead PI Ken Golden, University of Utah

N0001413MP20163: The Seasonal Evolution of Sea Ice Floe Size Distribution" – Lead PI Jacqueline A. Richter-Menge, USACE-CRREL

N0001414MP20126: Using discrete element modeling to improve resolved scale floe interaction modeling. Lead PI Arnold Song, USACE - CRREL

Imagery acquisitions and processing efforts are being coordinated closely with PI Richter-Menge's efforts to use similar imagery to track the seasonal evolution of floe size distribution and PI Song's efforts to conduct discrete element modeling. Imagery both from our remote sensing classifications and our planned UAV flights is being shared with PI Golden's efforts to track the evolution of melt pond geometry. Finally, the results of our efforts will produce a surface type classification dataset necessary for Perovich's work to assess the interaction of shortwave radiation with the summer ice cover.

An additional NSF-funded project (PI Polashenski) that will use the derived imagery products to track solar partitioning at the buoy sites has been selected for funding in FY15.

REFERENCES

- Frost VS, Stiles JA, Shanmugan KS, Holtzman JC, 1982. A Model for Radar Images and Its Application to Adaptive Digital Filtering of Multiplicative Noise. *IEEE Trans Pattern Anal Mach Intell* **4**:147-165. DOI: [10.1109/TPAMI.1982.4767223](https://doi.org/10.1109/TPAMI.1982.4767223).
- Osher SJ, Fedkiw RP, 2002. Level Set Methods and Dynamic Implicit Surfaces. *Springer-Verlag*. ISBN 0-387-95482-1.
- Rösel, A., L. Kaleschke, and G. Birnbaum (2012), Melt ponds on Arctic sea ice determined from MODIS satellite data using an artificial neuronal network, *Cryosphere* **6**, 1–19, doi:10.5194/tc-6-1-2012.
- Zakhvatkina NY, Alexandrov VY, Johannessen OM, Sandven S, Frolov IY, 2013. Classification of Sea Ice Types in ENVISAT Synthetic Aperture Radar Images. *IEEE Trans Geosci Remote Sens* **51**:2587-2599. DOI: [10.1109/TGRS.2012.2212445](https://doi.org/10.1109/TGRS.2012.2212445).

PUBLICATIONS

Polashenski, C., Eli Deeb, Christie Wood, Jackie Richter-Menge, Don Perovich, Karen Frey, and Melinda Webster, Remote Sensing of Meter-Scale Sea Ice Morphological Properties, IGS Sea Ice Symposia, Hobart, Tasmania March 2014 - **was not presented due to federal conference travel restrictions.**

Stwertka, C., C. Polashenski, E. Deeb, A. Arnsten, D. Perovich, Seasonal evolution of melt pond characteristics derived from Worldview and Quickbird imagery, AGU Fall Meeting 2014.

Istomina, L, G. Heygster, M. Huntemann, P. Schwarz, G. Birnbaum, C. Polashenski, D. Perovich, E. Zege, A. Malinka and A. Prikchach, The melt pond fraction and spectral sea ice albedo retrieval from MERIS data: validation and trends of sea ice albedo and melt pond fraction in the Arctic for years 2002-2011, *The Cryosphere* [submitted], 2014.

HONORS/AWARDS/PRIZES

Don Perovich, USACE-CRREL, AGU Fellowship Award, American Geophysical Union.